ISBN: 978-3-95450-236-3 ISSN: 2673-7027 doi:10.18429/JACoW-eeFACT2022-WEYAT0103

STUDIES AND POSSIBLE MITIGATION OF ELECTRON CLOUD EFFECTS IN FCC-ee

F. Yaman*,[1], İzmir Institute of Technology, İzmir, Türkiye
F. Zimmermann, CERN, Geneva, Switzerland
[1]also at STFC, Sci-Tech Daresbury, UK

Abstract

In this work, we present numerical results for the electron cloud build-up and mitigation studies considering Arc Dipole and Drift sections of the FCC-ee collider. We report the central electron density that could be reached by minimising secondary electron contributions and the photoelectron generation rates in order to achieve e^- densities lower than the single-bunch instability threshold, considering the baseline beam parameters. Additionally, simulation results revealing the behavior of electron-cloud formations for various SEY values, photoemission rates, vacuum chamber radii, and bunch spacings are included. In the last section, we discuss initial investigations to clean residual electrons after the beam pass.

INTRODUCTION

The FCC-ee, which is designed for performing precision measurements at each of several different collision energies between 88 and 365 GeV, is the first stage of the FCC project hosted by CERN [1, 2]. The design achieves a high luminosity with an e^+e^- circular collider of circumference $\approx$ 90 km, for the arcs of which we shall analyze electron cloud build-up scenarios. The exponential generation of electrons which may occur when the primary e^- hit the pipe walls, could cause beam loss, emittance growth, trajectory change, and wakefields [3,4]. The primary sources of the electrons in the accelerators and storage rings are photoemission, ionization of residual gases, and strikes of strayed beam particles to the beam pipes. For detailed investigations of the electron cloud mechanism, we employ PyECLOUD [5] to perform two-dimensional electrostatic particle in cell simulations. In the computations, the Furman-Pivi secondary electron yield model for copper, see Refs. [6, 7] and ECLOUD model based on laboratory measurements at CERN for the copper surface of the LHC [8, 9] are used.

MACHINE & SIMULATION PARAMETERS

We consider the machine and beam parameters which are given in Table 1 for the build-up simulations. Additionally, also the drift region, circular beam pipe radius 30 mm and 35 mm, bunch spacings 25 ns, 30 ns and 32 ns, total secondary emission parameter SEY = $\{1.1, 1.2, 1.3, 1.4\}$, the number of primary electrons generated by a single positively-charged particle per unit length $n'_\gamma = \{10^{-3}, 10^{-4}, 10^{-5}, 10^{-6}\}$ m^{-1} are scanned for the FCC-ee collider arcs. As a result, we obtain electron densities at the center of the vacuum chamber during 150 bunch passes where an average of all minimum density values is calculated to compare with the single-bunch instability threshold. The latter can be estimated as [12, 13]

$$\rho_{\rm thr} = \frac{2\gamma Q_s \omega_e \sigma_z / c}{\sqrt{3} K Q r_e \beta_y C} , \quad (1)$$

where

$$\omega_e = \left(\frac{N_b r_e c^2}{\sqrt{2\pi}\sigma_z \sigma_y (\sigma_x + \sigma_y)} \right)^{1/2} , \quad (2)$$

$K = \omega_e \sigma_z / c$, $Q = \min(\omega_e \sigma_z / c, 7)$, see Ref. [11].

Table 1: Simulation parameters for the simulations of electron-cloud evolution in an arc dipole, corresponding to collisions at 4 interaction points [10, 11].

Parameter	FCC-ee Collider Arc Dipole
beam energy [GeV]	45.6
bunches per train	150
trains per beam	1
r.m.s. bunch length [mm]	4.32
hor. r.m.s. beam size [μm]	207
vert. r.m.s. beam size [μm]	12.1
external magnetic field [T]	0.01415
bunch population N_b [10^{11}]	2.76
circumference C [km]	91.2
chamber radius r_0 [mm]	35
momentum compaction factor α_C [10^{-4}]	0.285
synchrotron tune Q_s	0.037
average beta function β_y [m]	50
threshold density ρ_{thr} [10^{12} m^{-3}]	0.043

NUMERICAL RESULTS

Firstly, Figure 1 displays minimum electron densities for a case without any secondary emission (SEY $\approx$ 0) and for a more realistic scenario (SEY = 1.1), considering a photoelectron rate of $n'_\gamma = 10^{-6}$ m^{-1}/e$^+$ and 32 ns bunch spacing. The former results for the arc dipoles reported in Ref. [11], even though the longitudinal rms bunch length, bunch population, and transverse beam sizes) had different

* fatihyaman@iyte.edu.tr

ISBN: 978-3-95450-236-3 ISSN: 2673-7027 doi:10.18429/JACoW-eeFACT2022-WEYAT0103

values (namely 3.5 mm, 2.8×10^{11}, 120 µm and 7 µm, respectively), still resemble those for the current parameters. For instance, in both old and new simulations, the minimum center density is $\approx 2\times10^{7}$ m^{-3} for SEY $\approx$ 0, and the maximum value $\approx 5\times10^{8}$ m^{-3} for SEY=1.1, for both SEY models.

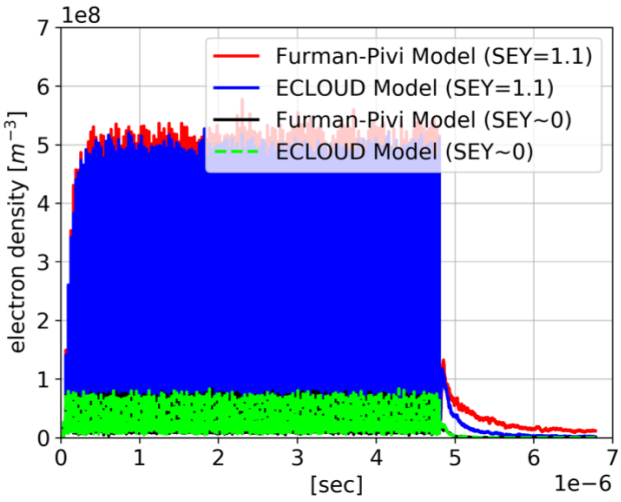

(a) e^- densities at the center of the vacuum chamber

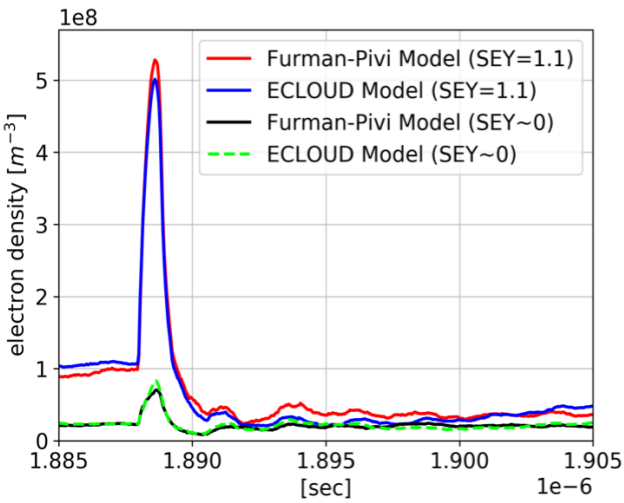

(b) variations of e^- densities during and after a bunch pass

Figure 1: Electron density for $n'_\gamma = 10^{-6}$ m^{-1} as a function of time, in the FCC-ee positron arc dipoles for Z pole operation.

For SEY=1.1, the Furman-Pivi and ECLOUD models for the secondary emission also yield similar results for the field-free regions, as is shown in Fig. 2, which was prepared by keeping the same parameters used for the previous example except for the external magnetic field, which is set to zero. However, a slight increase in the maxima of the oscillations can be noticed for the Furman-Pivi SEY model result. This behavior is expected according to our experience from past numerical experiments, since the Furman-Pivi model tends to yield higher electron density values. Furthermore, by comparing Figs. 1 and 2, we conclude that 0.01415 T an external magnetic field of 142 G, results in $\approx$ 2.5 times lower electron densities, for SEY=1.1 and $n'_\gamma = 10^{-6}$ m^{-1}.

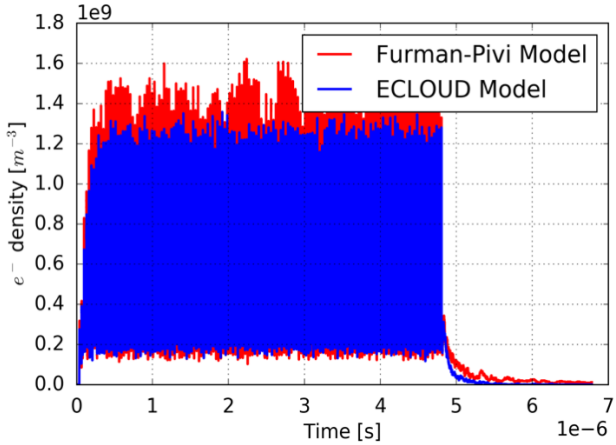

Figure 2: Electron density at the pipe center, as a function of time, for a bunch spacing of 32 ns, SEY=1.1, $n'_\gamma = 10^{-6}$ m^{-1}, without magnetic field.

Next, we examine the dependence of electron cloud build-up for a smaller beam pipe radius of 30 mm (instead of 35 mm), for 25 ns bunch spacing in the arc dipoles. Accordingly, in Fig. 3, the first row corresponds to the simulations with 30 mm pipe radius while the second row indicates results for 35 mm radius. For low SEY, the electron cloud is dominated by photoelectrons; therefore, a larger chamber reduces the average e- density, as can be seen from this figure. On the other hand, for SEY = 1.3 and SEY = 1.4, the multipacting dominates; in this case a larger chamber increases the multipacting and hence the maximum electron density. However, this behavior of the density maxima is now always followed by the more relevant density minima.

To compare the center densities with the threshold density $\rho_{thr} = 4.3\times10^{10}$ m^{-3} calculated via Eq. (1), the average of the minimum center-density values in the dipoles for the simulations with 25 ns bunches and two different radii is computed. Such average results obtained for various SEY values and photoelectron generation rates by employing both secondary emission yield models are depicted in Fig. 4. According to our simulation, the Furman-Pivi SEY model combined with the parameter $n'_\gamma = 10^{-3}$ m^{-1}, yields an electron density at the pipe center which exceed the threshold for both chamber radii. However, we obtain electron densities lower than the threshold by employing $n'_\gamma = 10^{-4}$ m^{-1} for all SEY values in the explored parameter range, up to SEY=1.4, although the density value for SEY = 1.4 with the Furman-Pivi model is still close to the threshold density, see Fig. 4 (b), so that the safety margin is small.

Our last numerical experiment is devoted to clearing the residual electrons with a single satellite bunch following a regular bunch train. In Ref. [14], Ruggiero and Zhang reported that a significant reduction of the beam-induced heat load can be obtained, for the case of the LHC, by choosing an optimum satellite bunch intensity and distance from the

ISBN: 978-3-95450-236-3 ISSN: 2673-7027 doi:10.18429/JACoW-eeFACT2022-WEYAT0103

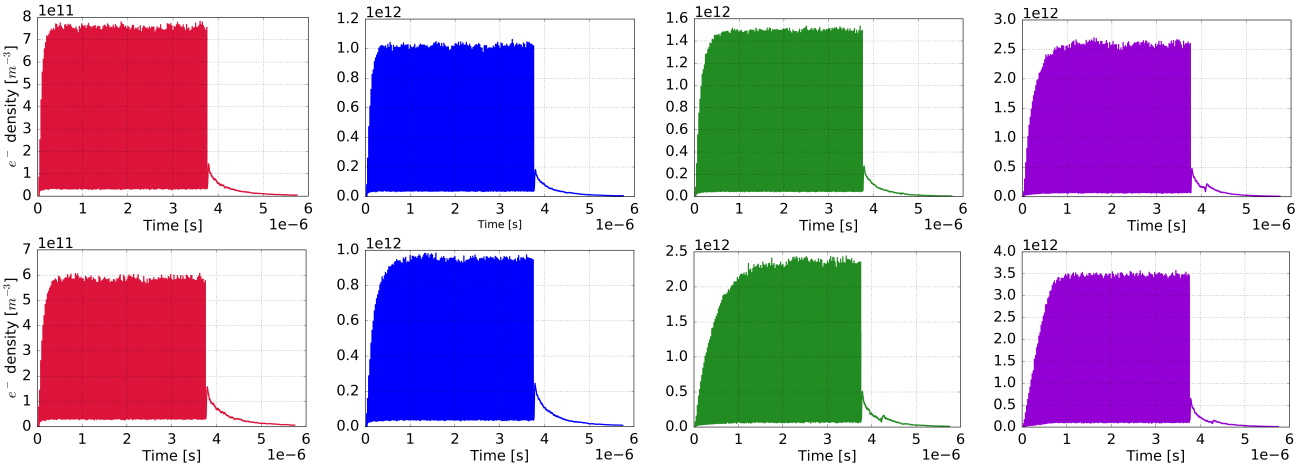

(a) SEY=1.1 (b) SEY=1.2 (c) SEY=1.3 (d) SEY=1.4

Figure 3: Electron density in the arc dipoles for bunch spacing:25 ns, SEY model:Furman-Pivi, $n'_\gamma = 10^{-3}$ m^{-1}, comparing chamber radii of 30 mm (top), and 35 mm (bottom)

.

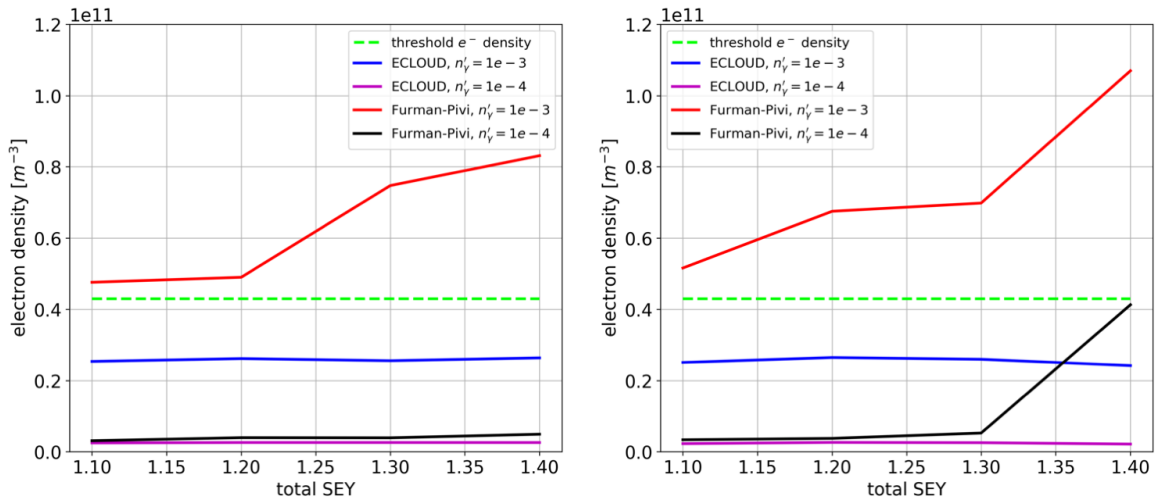

(a) chamber radius:30 mm (b) chamber radius:35 mm

Figure 4: Effect of the vacuum chamber radius for 25 ns spacing in the arc dipoles.

preceding nominal bunches. For the FCC-ee, we consider bunches at 30 ns spacing bunches with a bunch population of $N_b = 2.76\times10^{11}$ and the strongest secondary and photoemission parameters, namely SEY = 1.4 $n'_\gamma = 10^{-3}$ m^{-1} in addition to the Furman-Pivi model in the drift region. With this set of parameters, electron densities reach $\approx 1.75\times10^{13}$ m^{-3} during the bunch passes and sustain a electron density at the level of $\approx 10^7$ m^{-3} at the center of the beam pipe.

In Fig. 5, we examine the possibility of clearing the electrons left behind after the last bunch passes, in the drift region via an additional satellite bunch, whose populations is varied in between $10^4 - 10^{12}$ positrons. The satellite bunch was placed 15.45 ns behind the latest bunch in the train. At the distance of 15.45 ns the central electron density assumes a local minimum value. A significant increase of the electron density occurs for the largest satellite bunch population $N_b = 10^{12}$, in the parametric scan [15]. Otherwise, all other satellite bunches with different populations help to reduce the residual electron density. Trailing bunches with lower charges accomplish a more significant clearing of electrons [16] at the beginning. However, after a sufficiently long time, the center densities all converge to similar values, e.g., to $\approx 10^7$ m^{-3} about 20 µs after the train passage, including for the case without any trailing bunch.

CONCLUSION

In this study, we have reported results of electron-cloud build-up simulations with various combinations of SEY and photoelectron generation rates for the FCC-ee collider arc dipole beam pipe. The minimum attainabble electron density with negligible secondary emission in the dipole region is obtained as $\approx 2 \times 10^7$ m^{-3}. Furthermore, the evolution of the center electron density levels as a function of time

ISBN: 978-3-95450-236-3 ISSN: 2673-7027 doi:10.18429/JACoW-eeFACT2022-WEYAT0103

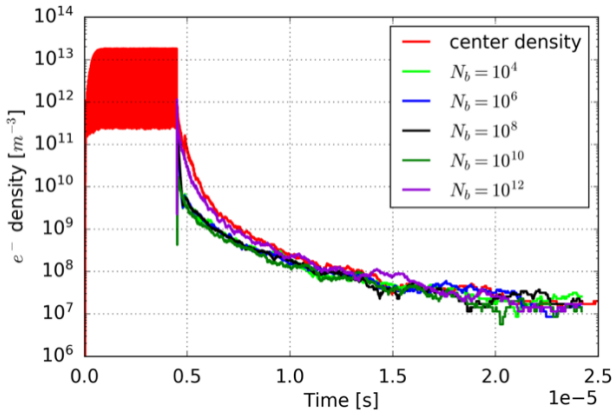

Figure 5: Mitigation tests via single trailing bunch in Drift

during several bunch passafes agree well, using either the ECLOUD or the Furman-Pivi model for the second amission yield, when considering the longest bunch spacing (32 ns) with the lowest SEY (1.1) and photoemission (10^{-6} m^{-1}), in our parameter scan for dipole and drift regions. The effect of the circular beam pipe radius is presented for 25 ns bunches. Reducing the vacuum chamber radius from 35 to 30 mm can helps suppress the electron-cloud formation.

Combining the results of Refs. [11, 15, 17], we conclude that, in order to keep minimum center electron densities lower than the single bunch instability threshold for both dipole and field-free regions, the condition $n'_\gamma < 10^{-3}$ m^{-1} should be satisfied independently of the SEY model, within the entire range of scanned beam and machine parameters, total SEY values, bunch spacings and pipe radii.

More specifically, for the dipole region, only $n'_\gamma = 10^{-3}$ m^{-1} combined with total SEY starting from 1.1 up to 1.4 of the Furman-Pivi model yields central densities larger than the threshold considering 30 mm or 35 mm circular beam pipe radius and any of 25 ns, 30 ns and 32 ns bunch spacings.

On the other hand, e^- density values at center of the vacuum chamber obtained with either ECLOUD or Furman-Pivi SEY models in the range of total SEY = 1.1–1.4 for $n'_\gamma = 10^{-3}$ m^{-1}, exceed the threshold level in the drift region. Additionally, as a particular case, for 35 mm pipe radius, the combination of $n'_\gamma = 10^{-4}$ m^{-1} with the total SEY = 1.4 of the Furman-Pivi model also leads to a density above the threshold.

It is worth noting that preliminary simulation results indicate the possibility of reaching $n'_\gamma \leq 10^{-4}$ m^{-1} by adding winglets and the photon absorbers to the vacuum chamber, see Ref. [18].

In the last part of the numerical section we presented initial results for clearing the residual electrons after the passage of a bunch train with a special single trailing bunch, demonstrating that such low-charge satellite bunches reduce the electron density, during several µs. This is of practical interest, since the separation of bunch trains for the FCC-ee Z running mode, will be of order 1–2 µs. For distances larger than about 5 µs the simulated density value converges to the one obtained without satellite bunch.

REFERENCES

[1] A. Abada *et al.* (edited by M. Benedikt *et al.*), "FCC-ee: the lepton collider, future circular collider conceptual design report volume 2", *Eur. Phys. J. Spec. Top.*, vol. 228, p. 261, 2019. 10.1140/epjst/e2019-900045-4

[2] A. Abada *et al.* (edited by M. Mangano *et al.*), "FCC physics opportunities, future circular collider conceptual design report volume 1", *Eur. Phys. J. C.*, vol. 79, p. 474, 2019. 10.1140/epjc/s10052-019-6904-3

[3] M. A. Furman and G. R. Lambertson, "The electron cloud effect in the arcs of the PEP-II Positron Ring", Report Nos. LBNL- 41123/CBP Note-246 and KEK Proc. 97-17, p. 170, 1997.

[4] F. Zimmermann, "A simulation study of electron-cloud instability and beam induced multipacting in the LHC", LHC-Project-Report vol. 95, 1997.

[5] PyECLOUD, https://github.com/PyCOMPLETE/PyECLOUD

[6] M. A. Furman and M. T. F. Pivi, "Probabilistic model for the simulation of secondary electron emission", Abbreviation Title *Phys. Rev. Spec. Top. Accel. Beam*, vol. 5, p. 124404, 2002. 10.1103/PhysRevSTAB.5.124404

[7] E. G. T. Wulff and G. Iadarola, "Implementation and benchmarking of the Furman-Pivi model for Secondary Electron Emission in the PyECLOUD simulation code", CERN, Geneva, Switzerland, Rep. No. CERN-ACC-2019-0029, 2019.

[8] B. Henrist, N. Hilleret, M. Jimenez, C. Scheuerlein, M. Taborelli, and G. Vorlaufer, "Secondary electron emission data for the simulation of electron cloud", in *Proc. ECLOUD'02*, CERN, Geneva, Switzerland, Apr. 2001, pp.75–78. doi:10.5170/CERN-2002-001.75

[9] G. Iadarola, "Electron cloud studies for CERN particle accelerators and simulation code development", PhD Thesis, Univ. Naples, CERN-THESIS-2014-047, 2014.

[10] K. Oide, D. Shatilov, *et al.*, "Collider performance, beam optics and design considerations baseline", FCCIS Deliverable Report FCCIS-P1-WP2-D2.1

[11] F. Yaman *et al.*, "Mitigation of electron cloud effects in the FCC-ee collider", *Eur. Phys. J. Tech. Instrum.*, vol. 9, p. 9, 2002. doi:0.1140/epjti/s40485-022-00085-y

[12] K. Ohmi, "Beam-beam and electron cloud effects in CEPC/FCC-ee", *Int. J. Mod. Phys. A*, vol. 31, no. 33, p. 1644014, 2016. doi:10.1142/S0217751X16440140.

[13] K. Ohmi, F. Zimmermann, and E. Perevedentsev, "Wake-field and fast head-tail instability caused by an electron cloud", *Phys. Rev. E*, vol. 65, p. 016502, 2001. 10.1103/PhysRevE.65.016502

[14] F. Ruggiero and X. Zhang, "Collective instabilities in the LHC: Electron cloud and satellite bunches", *AIP Conf. Proc.*, vol. 496, pp. 40–48, 1999.

[15] F. Yaman and F. Zimmermann, "Studies and possible mitigation of electron cloud effects in FCC-ee", in *Proc. 65th*

ISBN: 978-3-95450-236-3 ISSN: 2673-7027 doi:10.18429/JACoW-eeFACT2022-WEYAT0103

ICFA Advanced Beam Dynamics Workshop on High Luminosity Circular e+e- Colliders (eeFACT'22), Frascati, Italy, Sep. 2022, accompanying slides to paper WEYAT0103, this workshop.

[16] S. Veitzer (Tech-X), private communication, 2021.

[17] F. Yaman and F. Zimmermann, "Updates on the electron cloud build-up results for the FCC-ee", presented at the 159th FCC-ee Optics Design Meeting", 2022, https://indico.cern.ch/event/1205924/.

[18] F. Yaman, "Electron cloud densities at the center of the FCC-ee dipoles", presented at the 130th FCC-ee Optics Design Meeting, 2020, https://indico.cern.ch/event/982651/.